

# Practical and Sustainable Modification Method on Activated Carbon to Improve the Decolorization Process in the Acetaminophen Pharmaceutical Industry

Hongjie Liu, Yunrui Su, Cheng Liu, Andi Zhou, Xiaomeng Chu,\* Shaojie Liu,\* Xuteng Xing, and Erjun Tang



Cite This: *ACS Omega* 2021, 6, 5451–5462



Read Online

ACCESS |



Metrics & More

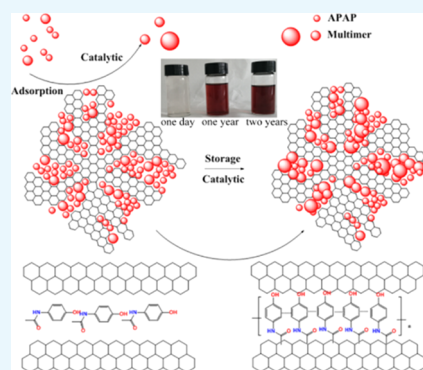


Article Recommendations



Supporting Information

**ABSTRACT:** Decolorization plays an important part in the industrial production of acetaminophen (APAP) drugs. The impurities generated from the APAP pharmaceutical industry decolorization refining process were primarily separated and purified, and their structures were determined by MS and  $^1\text{H}$  NMR technology. Then the catalytic effects of three samples of modified powdered activated carbon (PAC) on APAP in heterogeneous solution systems and the adsorption catalysis system were systematically investigated, which indicated that PAC catalyzed the APAP oxidative coupling side reaction and thus increased the impurities in the APAP product. The M-T-RAC (thermal regeneration PAC modified by ammonium sulfate) possessing more acidic surface groups can effectively inhibit this side reaction. Furthermore, according to the different catalytic results of O-T-RAC (thermal regeneration PAC modified by hydrogen peroxide) in solid–liquid catalytic and adsorption catalytic systems, we speculated that the multimer impurities were generated by the oxidative coupling reaction of APAP being oxidized to rated *N*-acetyl-*p*-benzoquinone (NAPQI) during decolorization, while free radical polymerization of APAP mainly occurred in the pores of the spent PAC. The pore textural structure and chemical properties of M-T-RAC were further characterized to ensure its feasibility of industrial application. The process of simulating industrial decolorization substantiated the excellent ability of M-T-RAC to inhibit side reactions. This study contributes to the development of green materials for sustainable recycling of activated carbon to reduce pollution and costs, and provides an effective advice for the pharmaceutical process.



## INTRODUCTION

Acetaminophen (APAP) is one of the most consumed analgesic and antipyretic medicines worldwide.<sup>1</sup> China is the largest producer of APAP in the world and exports tens of thousands of tons annually. The synthesis process of APAP is simple, which uses glacial acetic acid to acylate *p*-aminophenol. The decolorization section is an important part of APAP pharmaceutical engineering; the powdered activated carbon (PAC) is a commonly used decolorizing adsorbent in industrial production because of its high impurity removal rate and economy.<sup>2</sup> In order to protect the environment and reduce the costs, the spent PAC (SPAC) after decolorization needs to be recycled,<sup>3</sup> the commonly used regeneration method in the factory is the traditional thermal regeneration because of its simple regeneration crafts and because the equipment are relatively mature.<sup>2,4,5</sup> Other traditional regeneration methods include chemical regeneration<sup>6–8</sup> and steam regeneration.<sup>9,10</sup> The emerging new regeneration methods include microwave regeneration,<sup>11,12</sup> biological regeneration,<sup>13</sup> and photochemical regeneration.<sup>14–17</sup> However, these methods are met with limitations such as high energy consumption and carbon attrition,<sup>18</sup> higher cost,<sup>19</sup> and slow regeneration rates,<sup>20</sup> respectively.

The thermal regeneration activated carbon (T-RAC) is always employed to decolorize the crude APAP together with fresh PAC, and the T-RAC accounts for a larger proportion. The attendant main problem is that although the appearance of the APAP product meets the qualified standard, the content of colorless impurities is raised rapidly to even higher than that of crude APAP. On the other hand, the decolorizing power and refining ability of T-RAC obtained by thermal regeneration in the factory decreased for the collected SPAC from different batches with different storage times. All these issues can cause the quality fluctuation of the APAP final product and cause great difficulties to APAP quality control. Therefore, it is urgent to find out the reason for the increase of the impurities.

**Received:** November 21, 2020

**Accepted:** February 2, 2021

**Published:** February 15, 2021



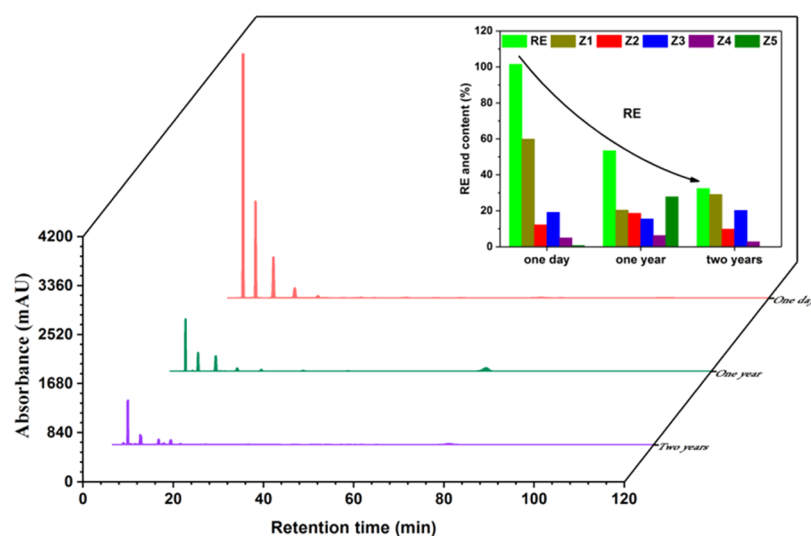


**Figure 1.** HPLC curves of ethanol extracts and chemical-thermal regeneration efficiency of SPAC at different storage times.

It has been reported that a phenolic compound could polymerize in activated carbon channels to form a polymer; this reaction occurred even in the absence of oxygen, and oxygen would accelerate the reaction.<sup>21–23</sup> However, the effect of this reaction on phenolic drugs was rarely reported. Vidic et al. found that phenolic adsorbates could polymerize on the surface of AC, and the presence of oxygen increased the adsorption capacity and irreversible adsorption capacity of ACs.<sup>24</sup> They also pointed that the metal content of AC surface did not affect the phenol polymerization catalyzed by AC; the key factor was the oxygen-containing functional groups on the AC surface.<sup>23</sup> Terzyk investigated the irreversible adsorption of phenol by AC; the results indicated that the irreversible adsorption of phenol was caused by the formation of strong complexes between phenol and the AC surface carbonyl groups and lactones, and the oxygen could react with the AC surface active sites to generate superoxide radicals, which further led to phenol polymerization.<sup>25</sup> Hence, the activated carbon can easily catalyze the oxidative coupling of phenolic compounds, which directly increase the irreversible adsorption of AC to phenol.

In view of the catalytic oxidative coupling reaction of activated carbon for phenolic compounds, the T-RAC should be modified to inhibit this adverse reaction. The common modification methods on AC include physical, chemical, and loading modification.<sup>26–30</sup> Chemical modification methods usually adopt chemical reagents to treat the surface of AC to change the surface chemistry and increase the content of the required functional groups, involving oxidation, reduction, and acid–base modification.<sup>31–34</sup> Meanwhile, the modification of activated carbon should not introduce new impurities, so as not to create new separation problems.

The practical objective of our study is to confirm the structures of the impurities, investigate the effect of PAC on the decolorization of crude APAP, and further to explore the mechanism of PAC with different surface chemistry properties by catalyzing APAP to produce impurities in decolorization side reactions. By modifying the T-RAC through chemical methods to change the surface chemical properties, we aimed to minimize the side reaction of decolorization and improve the regeneration efficiency of SPAC. Moreover, the changing of the pore textural structure and chemical

properties of the target modified AC (M-T-RAC) were also characterized and discussed. Finally, the simulating industrial decolorization experiments of modified ACs were carried out to ensure their practical applicability. This work will provide beneficial suggestions for the improvement of industrial APAP drug production.

## RESULTS AND DISCUSSION

**Separation and Purification of Impurity.** In order to accurately determine the structure and properties of the impurities in APAP products, the separation and purification of impurities were done first. As the content of impurities in the APAP product was very low, we enriched the impurities using the adsorbent SPAC that resulted from the decolorization process. The high-impurity-concentration solution was obtained after extraction and concentration, and the thin-layer chromatography (TLC) and high-performance liquid chromatography (HPLC) technology were used to analyze the purity of the impurities. Combined with <sup>1</sup>H NMR and MS analysis, the structures of the impurities were confirmed; five compounds, Z1–Z5, were determined in the extract, as shown in Table S1.

The molecular weights were determined by MS; compared to the 151 g/mol molecular weight of APAP, the monomers Z2 and Z3 were both 301 g/mol (M + H), which could be the APAP dimers. As shown in the <sup>1</sup>H NMR spectroscopy of Z2, two signals at 9.87 and 9.71 ppm, which were assigned to acetyl proton, appeared; however, only one hydroxyl proton resonance at 9.18 ppm emerged. All of these demonstrated that the monomer Z2 was the dimeric product of APAP formed by the C–O–C coupling reaction. However, in the Z3 <sup>1</sup>H NMR spectroscopy, only one acetyl proton peak was found and the number of protons belonging to the phenolic hydroxyl group was 2, as calculated by the integral ratio, which indicated that the Z3 monomer was the dimer of APAP formed by the C–C coupling reaction. Using the same inference procedure, combined with the results of HPLC, MS, and <sup>1</sup>H NMR spectroscopy, the Z4 monomer could be inferred as the trimeric APAP and Z5 monomer as the hexamer of APAP.

The daily output of SPAC produced in the decolorization section was low, while the traditional activated carbon

thermal regeneration processing technique in the factory had a large processing capacity; considering production cost, the SPAC would be concentrated and could be stored in multiple batches to regenerate. However, when the SPAC is stored for 2–3 months, the thermal regeneration efficiency would drop by 10–20%. Consequently, for the convenience of the operation, we chose chemical–thermal regeneration in the laboratory experiment to investigate the regeneration efficiency of SPAC and the changes of adsorbed substances in the SPAC pores during different storage times. As shown in Figure 1, with the extension of storage time, the regeneration efficiency of SPAC drops rapidly and the regeneration efficiency is only 32.4% for the SPAC stored for two years. From HPLC analysis of the eluted solution of aged SPAC, the content of Z5 (hexamer of APAP) reached 27.79% for one-year storage; however, it was not detected in the extract of SPAC after two years storage. Meanwhile, the content of soluble impurities in the extraction also decreases with the prolonged storage time. This indicates that during the storage of SPAC, Z3 monomer would be formed first and adsorbed by the PAC pores. As the storage time is extended, it will further polymerize to form higher-polymerization-degree monomers such as Z4 and Z5; until a larger-molecular-size multimer was generated that matched the PAC pore size or even larger, the desorption of these adsorbates was very difficult. This was the main reason for the decrease of SPAC regeneration efficiency. According to previous reports, AC can easily catalyze the oxidative coupling of phenolic compounds;<sup>21,35,36</sup> therefore, activated carbon may have a significant impact on the phenol oxidative coupling side reaction during the decolorization process, which can increase the impurity content in APAP finished products, and the irreversible adsorption capacity of PAC is also increased.

**APAP Oxidative Coupling Catalyzed by T-RAC.** In the preliminary stage, the factory engineers speculated that the impurities could be introduced by the raw materials or by the acylation side reaction, which leads to unqualified products. Through the quality tracking system, it was found that the content of impurities in the APAP products fluctuated into a certain regularity. In the factory, to control the cost, the PAC used for decolorization section was composed of fresh PAC and thermal-generation AC (T-RAC) (high percentage), which originated different batches of SPAC with different storage times. The impurity content of the APAP product rose rapidly when T-RAC was used in the decolorization process. However, the content of impurities could not be decreased in the APAP product even after adopting fresh PAC to again decolor the unqualified products. Combining the characteristics of the separated impurities Z2 and Z3, it could be inferred that the activated carbon-catalyzed APAP oxidative coupling was the main side reaction in decolorization engineering.

In order to verify this conjecture, we designed the catalytic reaction experiment of T-RAC to APAP under anaerobic conditions, which simulate the industrial operating environment. The blank-controlled trials with no T-RAC were also conducted simultaneously. As shown in Figure 2, the p-aminophenol decomposition product of APAP was not detected by the controlled reaction system, and the contents of Z2 and Z3 monomers increased slowly. However, with T-RAC in the reaction mixture, the contents of p-aminophenol, Z2, and Z3 increased significantly, and the content of p-aminophenol increased exponentially. Thus, AC can be an

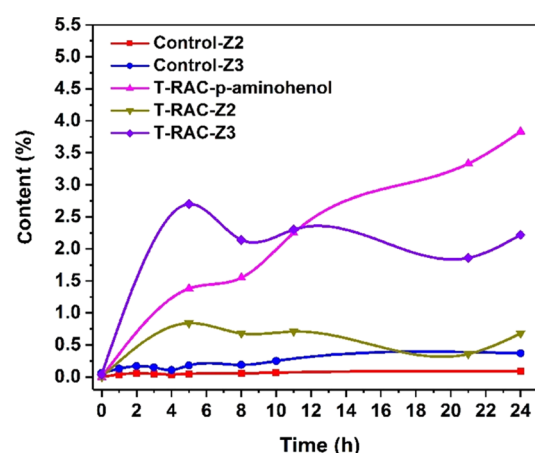


**Figure 2.** The content of impurities as a function of the time of T-RAC catalytic reaction detected by HPLC using the area normalization method.

important factor to induce the decomposition of APAP, which is unfavorable in decolorization engineering. The Z2 and Z3 contents showed a trend of first increasing and then decreasing; further polymerization reaction may occur in later stages to generate Z4 and Z5, which are easily adsorbed by the AC pores and cannot be detected in the reaction mixture. This result is consistent with the actual production experience because the decolorization time is always 10–20 min in practical operation and Z3 is the main impurity. Hence, the activated carbon with a variable surface chemical composition plays an important role in the oxidative coupling side reaction. The search for an effective activated carbon with specific chemical surface properties to inhibit decolorization side reactions is of utmost importance.

**Preparation of the Modified T-RAC.** To better comprehend the influence mechanism of the activated carbon surface chemistry on the decolorization side reaction, we fabricated three modified T-RAC samples with different surface chemistries using ammonium sulfate, hydrogen peroxide, and sodium borohydride, respectively. Quantification of the amount of acidic surface groups and basic surface groups in T-RAC, M-T-RAC, O-T-RAC, and R-T-RAC by the Boehm method is shown in Table 1. According to the

**Table 1.** Content of Oxygen Surface Functional Groups in T-RAC, M-T-RAC, O-T-RAC, and R-T-RAC Determined by the Boehm Method

sample	T-RAC	M-T-RAC	O-T-RAC	R-T-RAC
carboxylic groups/(mmol/g)	1.223	1.55	1.611	1.164
lactonic groups/(mmol/g)	0.537	0.438	0.293	0.071
phenolic groups/(mmol/g)	0.16	0.357	0.296	0.196
total acidity/(mmol/g)	1.920	2.345	2.200	1.431
total alkalinity/(mmol/g)	0.532	0.455	0.132	1.160
pH	6.21	5.20	3.08	6.98

results, the amount of surface acidic groups present in M-T-RAC increased to 2.345 mmol/g from 1.920 mmol/g after ammonium sulfate functionalization. After treatment by hydrogen peroxide, the surface functional groups of the obtained O-T-RAC were oxidized, the oxygen acid surface functional groups increased to 2.200 mmol/g, and the content of the basic functional groups was significantly

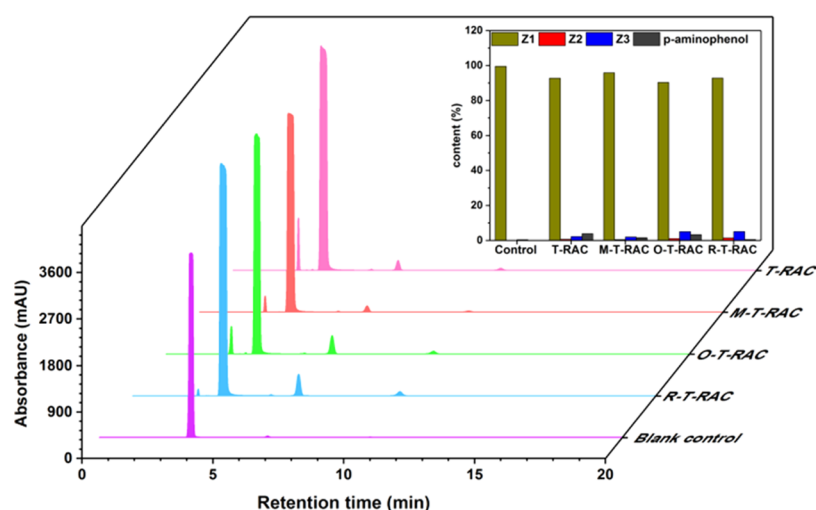


**Figure 3.** HPLC curves of the reaction solution after anaerobic catalysis of APAP for 24 h with different modified PAC samples.

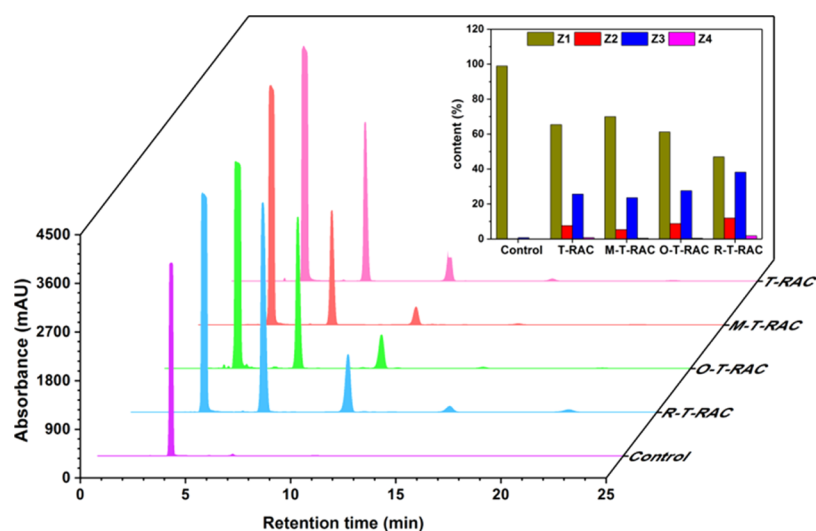


**Figure 4.** HPLC curves of the reaction solution after aerobic catalysis of APAP for 24 h with different modified PAC samples.

reduced, which was coincident with other reports.<sup>37,38</sup> On the contrary, the T-RAC was modified by the strong reducing reagent sodium borohydride (R-T-RAC); the oxygen surface functional groups were reduced<sup>39</sup> to obtain the increase of the basic functional groups as 1.160 mmol/g. The Fourier transform infrared (FT-IR) spectra of the modified activated carbons are shown in Figure S1; the peak at 3500  $\text{cm}^{-1}$  attributed to the typical stretching vibrations of the O-H groups in R-T-RAC became stronger compared to T-RAC; however, this band in the M-T-RAC curves was weaker. Compared to the T-RAC spectrum, the intensity of the carboxyl groups at 1599  $\text{cm}^{-1}$  was weaker in the R-T-RAC spectrum while it was stronger in M-T-RAC. All the FT-IR analyses are in agreement with the Boehm method results.

**Catalytic Reaction of PACs.** For further understanding the relationship between the chemical surface properties of PACs and the decolorization side reaction, the four PACs (T-RAC, M-T-RAC, O-T-RAC, and R-T-RAC) with different chemical surface properties were employed as catalysts to investigate their influence on the APAP decomposition and oxidative coupling reaction under anaerobic or aerobic conditions. Using APAP as substrate and under anaerobic atmosphere, as shown in Figure 3, the APAP decomposition

reaction can be inhibited to varying degrees, and R-T-RAC and M-T-RAC performed best, with the least p-aminophenol contents (0.5 and 1.58%) being detected. Regarding the APAP oxidative coupling reaction, the R-T-RAC with more basic surface groups shows excellent catalytic performance for the highest Z3 monomer content (5.05%) in its reaction filtrate. To our delight, the M-T-RAC possessing more acidic surface groups can effectively inhibit the APAP oxidative coupling reaction, and the contents of Z2 and Z3 are only 1.58 and 0.45%, respectively, which are much lower than those of the T-RAC reaction system. The APAP content was also maintained the highest in the M-T-RAC reaction system compared to other modified PACs. Therefore, in the anaerobic decolorization process, the M-T-RAC modified by ammonium sulfate modification can effectively inhibit the catalytic APAP oxidative coupling and decomposition reactions.

Before the practical decolorization engineering in the factory, hot steam is always employed to purge the decolorization tank to keep the air removal and to protect the APAP from being oxidized during the decolorization process. However, the air will inevitably be introduced during the feeding process, so we designed the catalytic reaction

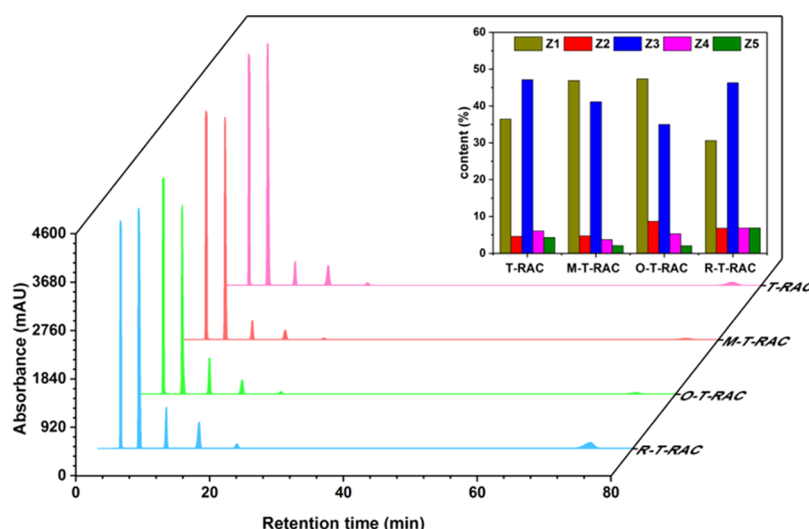


**Figure 5.** HPLC curves of the eluent after adsorption of APAP for seven days with different modified PAC samples.

under aerobic atmosphere to explore the effect of  $O_2$  on this reaction with four PACs; the results are shown in Figure 4. The p-aminophenol was not detected in any of the experimental solutions: not even in the T-RAC instance, which can catalyze the decomposition of APAP to generate a large amount of p-aminophenol in the anaerobic condition. It demonstrated that the  $O_2$  can effectively inhibit the APAP decomposition reaction. Compared with anaerobic catalytic experiments, the impurity contents were increased in all the reaction solutions; the Z3 content monomer had increased from 0.37% to 0.73% in the blank-controlled trials. Simultaneously, the contents of Z2 and Z3 monomers in all trials with PACs were increased dramatically, even the Z4 tetramer emerged, and it was proved that the  $O_2$  can accelerate the oxidative coupling reaction of APAP, similar to previously reported works.<sup>21,23</sup> Similar to the trend in anaerobic conditions, the contents of Z2 and Z3 were the highest (11.97 and 38.17%) and the APAP content was lowest (46.93%) in the R-T-RAC reaction system with more basic surface groups. Even under aerobic conditions, the M-T-RAC exhibited excellent inhibition of oxidative coupling reaction performance, because the Z2 and Z3 contents were only 5.33 and 23.59%, and the APAP was detected to be the highest (69.94%). To summarize, the PACs with more basic surface groups can promote the oxidative coupling reaction of APAP, and those with more acid surface groups can effectively inhibit this side reaction.

**Adsorption Catalysis Reaction.** On the basis of previous research, the APAP multimer will emerge from the stored SPACs with the extension of time. We carried out the adsorption catalysis reaction of these modified PACs for seven days, and the analytical HPLC results of the impurities in the eluate are shown in Figure 5. With prolongation of time all PACs strongly catalyzed the APAP oxidative coupling reaction in the inner pores, the content of APAP in all ethanol elutriants of the different PAC samples was less than 50%, and the M-T-RAC and O-T-RAC performed best in inhibition of the discoloration side reaction when carrying more acidic surface sites. It can be clearly observed that Z3 monomer was the main coproduct; however, interestingly, different from the heterogeneous catalytic reaction, more APAP multimers such as Z4 and Z5 were identified in the

adsorption catalysis reaction of the pore structure of PACs. This indicates that the activated carbon pore structure possesses stronger catalytic performance. The O-T-RAC exhibits relatively lowest catalytic performance by comparison with the heterogeneous catalytic reaction; this abnormal phenomenon suggests different catalytic mechanisms in the two catalytic systems.

In a valuable published work, Nematollahi et al. discussed about electrochemically generated *N*-acetyl-*p*-benzoquinone-imine (NAPQI) participating in different types of reactions based on the pH of solution and give the probable mechanism of the formation of APAP dimer.<sup>40</sup> Another constructive research was undertaken by Potter et al., who explored the polymerization of APAP catalyzed by horseradish peroxidase and isolated six types of products from the reaction mixture using semi-preparative HPLC.<sup>41</sup> Enzymatic oxidation of acetaminophen may occur by either a 1- or a 2-electron process to produce free radicals or NAPQI, respectively. In the solid-liquid catalysis reaction, the APAP oxidative coupling side reaction mainly occurred on the outer surface of the PAC; the negative ions and oxidation intermediates of APAP may be present in the reaction solution. Combined with the obtained results, the possible heterogeneous catalytic APAP oxidation mechanism was speculated, as shown in Scheme S1.

In the presence of activated carbon, the APAP can generate *N*-acetyl-*p*-benzoquinone imine NAPQI (3) and its phenolic hydroxyl can ionize a  $H^+$  to give anions (2) in water. The Michael addition reaction of anion 2 via C-alkylation to NAPQI (3) leads to dimer Z3.<sup>40</sup> The anion 2 can also attack the  $\beta$ -carbon atoms with low electron density of NAPQI (3) through electrophilic substitution to generate dimer ether Z2. The R-T-RAC having more basic groups will provide an alkaline environment, which can promote the phenolic hydroxyl ionization to give anion 2 and further lead to the generation of Z2 and Z3 monomers. More oxidizing functional groups were obtained after the T-RAC modified by hydrogen peroxide; then the O-T-RAC can easily facilitate the formation of the NAPQI (3) intermediate. Meanwhile, the  $O_2$  can directly oxidize APAP to produce NAPQI (3), which is the reason why the catalytic oxidative coupling reaction of PACs was intensified and the Z4 multimer even

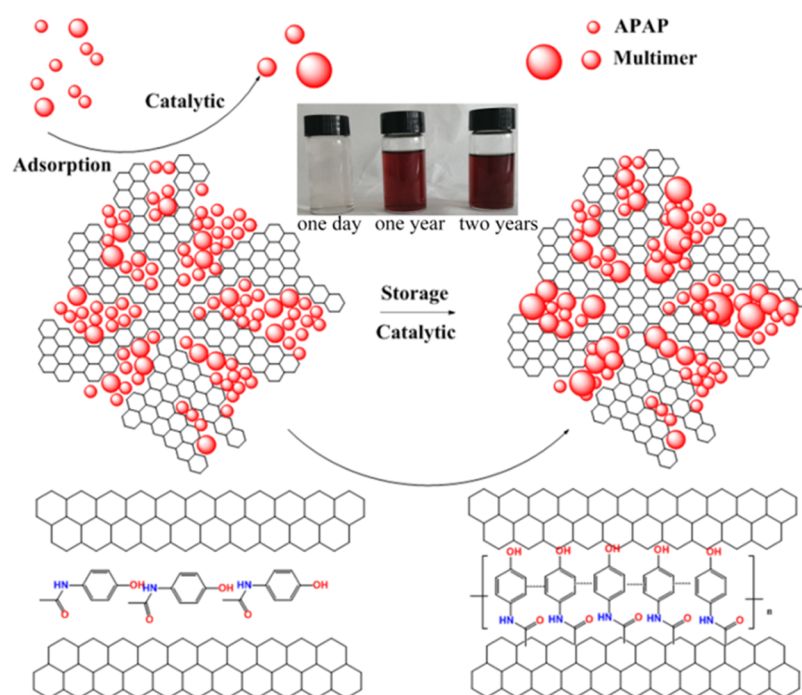


**Figure 6.** PAC-catalyzed APAP reaction polymerization in the pore channel.

appeared in the presence of  $O_2$ . After modification by ammonium sulfate, the acidic surface groups of M-T-RAC were increased and would ionize the  $H^+$  in solution,<sup>41–43</sup> providing an acidic environment that can suppress the generation of intermediate anion 2. The following high-temperature ( $600\text{ }^\circ\text{C}$ ) treatment could decompose the oxidizing functional groups; thus, the surface chemical property of M-T-RAC enables reduction of the catalytic activity and inhibits the APAP oxidative coupling side reaction.

In adsorption catalysis reaction, the O-T-RAC showed contrast catalytic performance with solid–liquid catalysis reaction, which is ascribed to the different catalysis mechanism in the PAC pore channels. In the pore channel structure of activated carbon materials, the inner functional groups initiate phenol to generate free radicals to trigger the free radical polymerization shown in Scheme S2. The APAP could convert into anion 2 and free radicals 4 and 5; two free radicals 5 could form dimer Z3; and 2 reacted with phenoxy 4 to give dimer Z2.<sup>44,45</sup> After modification by hydrogen peroxide, the PAC functional groups that promote radical generation were reduced, so the O-T-RAC could inhibit the pore internal oxidative coupling reaction the best.<sup>46</sup> Moreover, the absorbed APAP in the SPAC can polymerize into multimers such as Z4 and Z5 and even with higher polymerization degree, as shown in Figure 6. Multimers with larger molecular size will be difficult to desorb in the pores of activated carbon, which can block the channel structure, and the increasing boiling point and decomposition temperature of the polymers lead to difficulty of desorption even in the thermal regeneration under  $1200\text{ }^\circ\text{C}$ . The difference in SPAC storage time leads to changes in the T-RAC decolorizing performance, which was also the main reason for the obvious fluctuation of product quality after using T-RAC in the decolorization section. With all of these obtained results together, the M-T-RAC modified by ammonium sulfate can be the most suitable candidate to

inhibit the APAP oxidative coupling reaction during the decolorization and storage time, thereby improving the product equability and SPAC regeneration efficiency.

**Characterization of M-T-RAC.** The M-T-RAC as prepared by ammonium sulfate chemical modification showed excellent ability to inhibit the side reactions of oxidative coupling. From the perspective of industrial production cost, environmental protection, and equipment and technology requirements, the ammonium sulfate modifier is cheap and easy to get, and the treatment temperature of the modification process is also low relatively; hence, this modified T-RAC is appropriate to be used in the industrial APAP decolorization process. However, the PAC employed in the pharmaceutical process requires high quality, so the modification process must not introduce new pollutants. Therefore, we further characterized the pore structure and chemical properties of M-T-RAC by adopting SEM, EDX, BET, and adsorption isotherms.

Figure S2 depicts the SEM images of T-RAC and M-T-RAC. The porous system and well-developed pore morphology were observed on the surfaces of both T-RAC and M-T-RAC. After modification, under the activation of the modifier and at high temperature, the surface of the MA-T-RAC became smooth and the arrangement of the pore structure was also tighter and orderly, suggesting the surface impurities generated by carbon deposition were removed during the modification process.<sup>5</sup> EDX spectrum with the insets of elemental analysis was done for chemical characterization of the prepared T-RAC, M-T-RAC, R-T-RAC, and O-T-RAC as exhibited in Figure S3. The contents of the oxygen element of M-T-RAC and O-T-RAC are 16.54 and 15.49 wt %, higher than that of T-RAC (10.37 wt %) before modification, giving good agreement with the Boehm results. No significant changes of the content of the surface elements are observed for R-T-RAC compared with T-RAC, because the ketone groups and oxidizing functional groups were reduced by sodium borohydride, which will not influence the elemental

content changes. The contents of carbon and sulfur elements show a slight downward trend due to the interaction of ammonium sulfate and the surface groups of activated carbon at the high temperature.<sup>47</sup> Nitrogen element was not detected in T-RAC, M-T-RAC, O-T-RAC, and R-T-RAC, indicating that the modifying agents were completely decomposed after modification and no new impurities were introduced to T-RAC.

The N<sub>2</sub> adsorption–desorption isotherm and BJH pore size distribution displayed by the T-RAC, M-T-RAC, O-T-RAC, and R-T-RAC are given in Figure S4, all with type IV isotherm as per the IUPAC classification, which indicates the presence of the mesoporous structure. All the modification did not change the type of pore structure. Figure S4b represents the pore size distributions for T-RAC, M-T-RAC, O-T-RAC, and R-T-RAC, which clearly explains that the pore sizes of all the samples lie in the range 2–10 nm, out of which yet the pore volume with 2–4 nm pore diameter of M-T-RAC is slightly higher than that of T-RAC, even almost 1.7 times higher than those of O-T-RAC and R-T-RAC. The results obtained from BET analysis are shown in Table 2;

**Table 2.** Physical Properties of T-RAC and M-T-RAC

sample	$S_{\text{BET}}$ (m <sup>2</sup> /g)	$V_{\text{T}}$ (cm <sup>3</sup> /g)	$V_{\text{micro}}$ (cm <sup>3</sup> /g)	$V_{\text{meso}}$ (cm <sup>3</sup> /g)	$V_2 \leq d_4$ (cm <sup>3</sup> /g)	$D_p$ (nm)
T-RAC	1555.8	1.178	0.288	0.890	0.292	3.028
M-T-RAC	1589.3	1.174	0.246	0.928	0.341	2.955
O-T-RAC	1273.5	1.062	0.186	0.876	0.241	3.334
R-T-RAC	1185.4	1.016	0.150	0.866	0.238	3.428

although the micropore volume of M-T-RAC has decreased to 0.246 cm<sup>3</sup>/g from 0.288 cm<sup>3</sup>/g (T-RAC), the mesopore volume has increased to 0.928 cm<sup>3</sup>/g, which is higher than that of T-RAC (0.890 cm<sup>3</sup>/g). The micropore volumes of O-T-RAC and R-T-RAC samples, in contrast, were decreased dramatically to 0.186 and 0.150 cm<sup>3</sup>/g; the mesopore volume (0.876 and 0.866 cm<sup>3</sup>/g) is also somewhat below that of T-RAC. This demonstrates that the modified M-T-RAC pore size distribution is concentrated in the small-sized mesopores, and the decreased  $D_p$  values are beneficial to the physical adsorption of the Z2 and Z3 impurities monomer.

**Adsorption Isotherms.** To evaluate the effect of ammonium sulfate modification on the adsorption capacity of T-RAC, methylene blue (MB) was used to represent the colored impurities and dimers in the crude APAP. To observe whether phenol used as p-aminophenol may exist during APAP decolorization, we estimated the MB, APAP, and phenol maximum adsorption capacities of T-RAC and M-T-RAC by using adsorption isotherms. The fit of the Langmuir, Freundlich, and Temkin isotherm models to the experimental data provides information about the nature of adsorption, as shown in Figure 7. The adsorption isotherm parameters for MB, APAP, and phenol onto T-RAC and M-T-RAC are listed in Table 3. The Langmuir model was established according to the hypothesis that the adsorption on the adsorbent forms a monolayer, and the adsorption sites are uniformly distributed, ignoring the interaction between adsorbate molecules. The Langmuir isotherm equation ( $R^2 > 0.94$ ) fitted the MB and APAP adsorption experiment data better and the Freundlich isotherm equation, which assumes

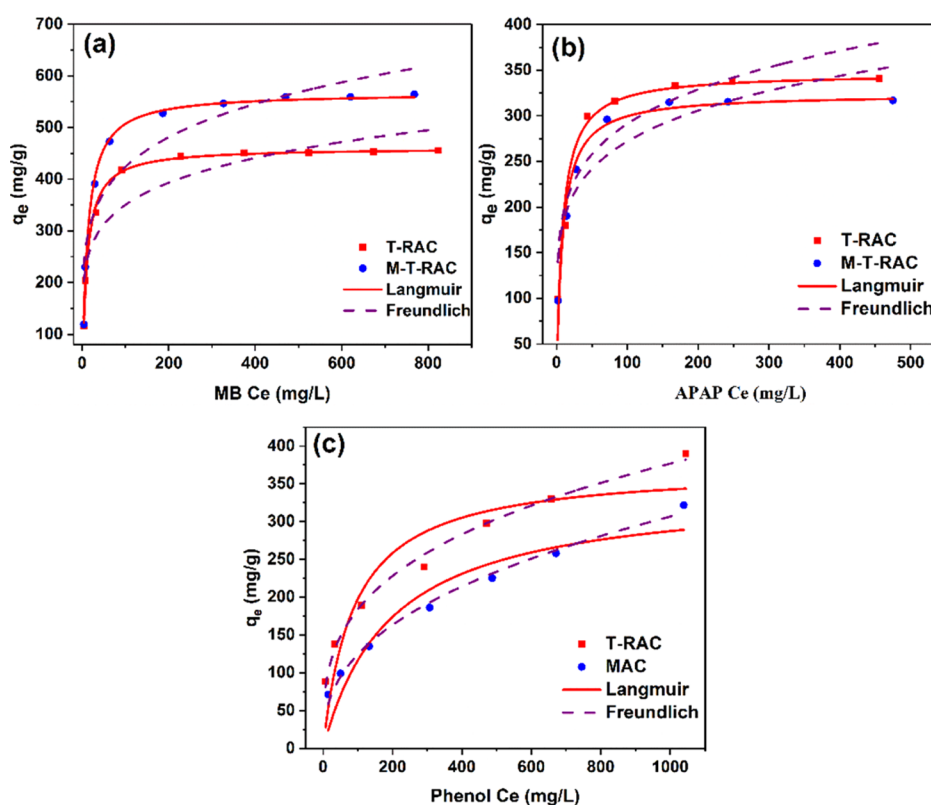


**Figure 7.** Adsorption isotherm (32 °C) of (a) MB; (b) APAP; and (c) phenol by T-RAC and M-T-RAC (concentration range of adsorbate: 75–1200 mg/L).

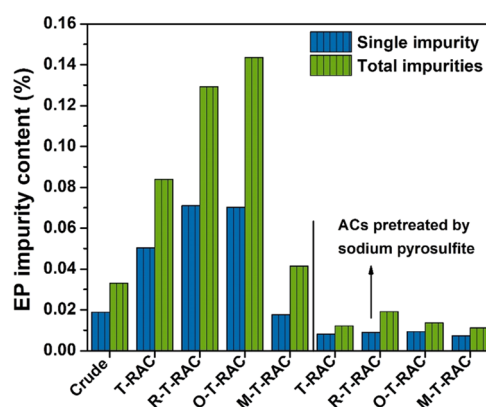
**Table 3.** Langmuir, Freundlich, and Temkin Constants for the Adsorption of MB, APAP, and Phenol on T-RAC and M-T-RAC

constants	T-RAC			M-T-RAC		
	MB	phenol	APAP	MB	phenol	APAP
	Langmuir Isotherm					
$K_L/(L/mg)$	0.0 983	0.0 113	0.1 234	0.0 844	0.0 051	0.1 229
$q_m$ (mg/g)	460.72	372.64	346.74	567.11	343.56	315.72
$R_L$	0.145	0.640	0.139	0.165	0.800	0.140
$R^2$	0.992	0.861	0.947	0.990	0.893	0.975
	Freundlich Isotherm					
$K_F/(mg/g)$	163.50	43.92	129.97	183.80	20.57	124.92
$1/n$	0.166	0.311	0.175	0.182	0.391	0.169
$R^2$	0.823	0.994	0.864	0.842	0.991	0.856

a heterogeneous adsorbent surface, matched the phenol adsorption data ( $R^2 > 0.99$ ).<sup>48–51</sup>

The maximum monolayer adsorption capacity ( $q_m$ ) of MB onto M-T-RAC determined from the Langmuir model is 567.11 mg/g, which is 23.1% higher than that onto T-RAC (460.7 mg/g) and is ascribed to the increased pore volume in the effective adsorption pore size range. Additionally, the  $R_L$  values of M-T-RAC and T-RAC are 0.165 and 0.145, respectively, indicating the favorability of the MB adsorption process. As the concentration of MB is less than 150 mg/L, the adsorption equilibrium model follows the Henry law, which implies that the removal rate of MB in this range can reach above 99%. Furthermore, the  $q_m$  values of APAP and phenol onto M-T-RAC were decreased from 346.74 and 372.64 mg/g onto T-RAC to 315.72 and 343.56 mg/g. Therefore, ammonium sulfate modification can improve the adsorption capacity of activated carbon on multimers such as Z2, Z3, and colored impurities and reduce the adsorption capacity of APAP products, which is favorable for the decolorization engineering.

**Decolorization of Crude APAP.** The impurity content of crude APAP complies with the EP standard (single impurity < 0.05%, total impurities < 0.1%). The main purpose of decolorization is to remove colored impurities and make both the appearance and purity of the finished product qualified. In the actual industrial decolorization process, a small amount of sodium pyrosulfite was added into the filtrate before crystallization to prevent the APAP from being oxidized. However, during the decolorization with PAC, no sodium pyrosulfite was added into the system. For further estimation of the modified activated carbon practical decolorization performance, we employed these four PACs in the simulated decolorization process and compared the content of impurities of the two cases with and without pretreatment of sodium pyrosulfite; the results are shown in Figure 8. In the case of PACs without pretreatment by sodium pyrosulfite, the impurities content of the product increased and even did not meet the quality requirements. Consistent with the experimental results of the catalytic reaction, the content of APAP impurity increased significantly by using R-T-RAC and O-T-RAC; however, the M-T-RAC effectively decreased the impurity content. Therefore, the PAC-catalyzed APAP oxidative coupling side reaction can directly affect the quality of the product. In order to prevent APAP oxidation and inhibit the side reactions (reduce the production of NAPQI) during the decolorization process, we pretreated the PACs with sodium pyrosulfite before decolorization. We could clearly see that the impurity

**Figure 8.** Decolorization results (EP standard) of crude APAP products by AC samples with and without pretreatment of sodium pyrosulfite.

contents were decreased dramatically, and the sodium pyrosulfite used during the decolorization process sufficiently inhibited the side reaction. However, the PAC may still catalyze the APAP oxidative coupling reaction because the impurity content increases with O-T-RAC and R-T-RAC. In actual industrial production, the large amount of addition of sodium pyrosulfite during decolorization can significantly reduce the filtration rate of the PACs. Therefore, only a small amount of sodium pyrosulfite was used to pretreat the PAC, which cannot completely inhibit the production of NAPQI. The modification of PAC with ammonium sulfate before decolorization can effectively reduce the usage amount of PAC and reduce the impurities in the product APAP, because the catalytic performance of the decolorizing PAC is the main factor affecting product quality. Based on the above analyses, the M-T-RAC is the best candidate to inhibit the side reaction during industrial decolorization, avoid irreversible adsorption and excessive polymerization in the PAC pores, improving the regeneration efficiency, and effectively maintain the decolorization capacity of the PAC.

## CONCLUSIONS

This article aims to solve the practical problem of the impurity content in APAP products rising sharply after decolorization encountered in the industrial decolorization engineering of acetaminophen and gives an in-depth insight into the activated carbon modification for decolorization. Through the purification of the impurities in APAP products by the enrichment and separation method, they were confirmed to be the APAP multimers by MS and <sup>1</sup>H NMR



analysis. With the time extending, the stored spent thermal regeneration activated carbon (SPAC) showed a decreased regeneration efficiency and produced high-order multimers that were difficult to desorb. Results of the catalytic reaction experiment of T-RAC to APAP show that PAC can catalyze the oxidative coupling and decomposition side reaction of APAP. The surface chemistry of the PAC can significantly influence the catalytic activity and the M-T-RAC that has more acidic surface groups can effectively inhibit this side reaction. O-T-RAC showed different catalytic performances with solid–liquid catalysis reaction and adsorption catalysis reaction, indicating different catalytic mechanisms. In the heterogeneous system the polymerization was mainly ascribed to the generation of the oxidation intermediate NAPQI of APAP and in the adsorption catalysis system it was a free radical reaction. The characterization of the pore structure and chemical properties of M-T-RAC by adopting SEM, EDX, BET, and adsorption isotherms demonstrated that the ammonium sulfate modification of T-RAC was favorable for the decolorization engineering. In the simulated decolorization, the M-T-RAC showed the feasibility to be employed in the practical APAP industrial decolorization.

## EXPERIMENTAL PROCEDURES

**Materials.** All reagents, such as hydrogen peroxide (30 wt %), sodium borohydride, ammonium sulfate, petroleum ether, ethyl acetate, methylene blue, sodium pyrosulfite, sodium hydroxide, methanol, and ethanol (95 wt %), were of analytical grade and purchased from Sinopharm Chemical Reagent Co., Ltd., China. The spent PAC (SPAC), thermal regeneration activated carbon (T-RAC), and crude APAP products are from Jiheng (Group) Pharmaceutical Co., Ltd. (Hebei, China).

**Separation and Purification of Impurity.** The SPAC from APAP decolorization section was stored in a dark place for 7 days; after that the SPAC (200 g) and 300 mL of ethanol (95%) were added to a 1 L round-bottomed flask and the mixture was stirred at 78 °C for 3 h. After filtration, the collected filtrate was concentrated by rotary evaporation to get a saturated solution of desorbents; the aqueous phase was extracted with ethyl acetate; finally, the combined organic solvent was concentrated under reduced pressure to afford the extractors. The extractors were separated through thin-layer chromatography (TLC) and silica gel column chromatography.

### Preparation of Modified Activated Carbons.

- (i) Ammonium sulfate modified T-RAC (M-T-RAC): In a typical procedure, 200 g of T-RAC and 1 L of ammonium sulfate aqueous solution (100 g/L) were added to a 2 L conical flask in order. The resulting mixture was stirred at room temperature for 30 min and then allowed to stand for 24 h. After filtration, the residual solid was washed thoroughly with ultra-pure water for 3 times and oven-dried at 105 °C for 4 h. The obtained activated carbon was placed in a tubular furnace and heated at 10 °C/min from ambient temperature to 600 °C and then kept at 600 °C for 3 h. After that, the tubular furnace was cooled down to room temperature and the resulting product was designated as M-T-RAC.
- (ii) Sodium borohydride modified T-RAC (R-T-RAC):<sup>39</sup> Briefly, 5 g of sodium borohydride (5 g) in ethanol (20

mL) was added dropwise to an evenly stirred heterogeneous solution of T-RAC (15 g) in ethanol (50 mL); then the reaction mixture was heated to 75 °C and kept at this temperature for 3 h. After filtration, 0.005 mol/L hydrochloric acid and hot water were used to wash the filter cake successively, and the product was vacuum dried at 100 °C for 48 h to afford the reductive thermal recycled carbon (R-T-RAC).

- (iii) Hydrogen peroxide modified (O-T-RAC):<sup>37</sup> Fifteen grams of TRAC was dispersed uniformly in 50 mL of ultra-pure water by ultrasonic vibration; then 15 mL of hydrogen peroxide (30%) was added dropwise to the mixture and stirred at room temperature for 3 h. Subsequently, the modified carbon was filtered and washed thoroughly with ultra-pure water for 4 times. After oven drying at 120 °C for 24 h, the oxidation thermal recycled carbon was obtained and was named as O-T-RAC.

### Catalytic Reaction of PACs.

- (i) Heterogeneous catalytic reaction (anaerobic or aerobic): The anaerobic heterogeneous catalytic reaction of PACs was carried out in a 500 mL round-bottomed flask containing 250 mL of ultra-pure water, APAP (10 g, 0.04 g/mL), and PAC (T-RAC or modified T-RACs, 1 g, 0.004 g/mL). The reaction mixture was stirred uniformly at 100 °C under nitrogen atmosphere, and the content of substance in the reaction solution was determined by HPLC technology after filtering using an organic filter at regular intervals. For a control experiment, the reaction without T-RAC also proceeded under the same conditions. The aerobic heterogeneous catalytic reaction of PACs was performed in the same way but without N<sub>2</sub>, and the reaction temperature was adjusted to 95 °C.
- (ii) Adsorption catalysis reaction: In a 100 mL Erlenmeyer flask, PAC (TRAC or modified T-RACs, 5 g) and crude APAP (15 g) were dissolved in 50 mL of ultra-pure water; the mixture was stirred and heated to 100 °C for 15 min. After filtering, the filter cake was sealed in a plastic bag, drained of air, and placed in the dark for 7 days. Then, the adsorbate in PAC was extracted using 60 mL of ethanol at 78 °C for 3 h, and the organic solvent was removed by rotary evaporation. The content of substance in the extract was monitored by HPLC.

**Bath Adsorption Studies.** Bath adsorption was implemented in conical flasks of 250 mL containing 0.05 g of PACs and 100 mL of adsorbate (APAP, MB, phenol) solutions with different concentrations ranging between 75 and 1200 mg/L. A mechanical shaker was employed to shake the flasks containing the mixtures at 25 °C with predetermined times of 2–6 h and an agitation speed of 120 rpm. Subsequently, the mixtures were filtered using a medium-speed qualitative filter paper, and the concentrations of adsorbates remaining in the solution were determined using a UV–vis spectrophotometer (YoKe, UV1900) at the calibrated maximum wavelengths of 270, 665, and 245 nm for phenol, MB, and APAP solutions, respectively.<sup>17</sup> The solution of MB was prepared using a phosphate buffer solution with pH ≈ 7; the solution of APAP and phenol was prepared in distilled water. The amount adsorbed at the equilibrium ( $q_e$ , mg/g) was calculated by using the following equations

$$q_e = \frac{(C_0 - C_e)V}{M} \quad (1)$$

where  $C_0$  and  $C_e$  are the initial adsorbate concentration (mg/L) and the equilibrium adsorbate concentration (mg/L), respectively,  $q_e$  is the adsorption capacity (mg/g),  $V$  is the volume of the solution (L), and  $M$  is the mass of adsorbent (g).

**Crude APAP Decolorization.** In a 100 mL flask, the crude APAP (13.8 g) were dissolved in ultrapure water (16.9 mL) under a nitrogen flow at 80 °C. Then, 3.67 g of activated carbon solution (27.2 wt %, the solvent was ultrapure water or 2 g/L sodium pyrosulfite aqueous solution) was added to the crude APAP solution and heated up to 100 °C. The decolorization was completed 15 min later, and the activated carbon was filtered out while the reaction solution was hot. Finally, the collected filtrate was heated up to 90 °C with addition of 0.33 g of sodium pyrosulfite. With the temperature of the solution decreasing, the APAP crystallized and was vacuum dried at 105 °C for 8 h. The content of impurities in the APAP product was determined by HPLC.

**Characterization and Measurements.** Using  $^1\text{H}$  NMR spectroscopy (Bruker, Avance 500 MHz) and a mass spectrometer (MS, Varian, 500-MS), the structures of the impurities were investigated. High-performance liquid chromatography (HPLC, ThermoU3000) was employed for the quantitative determination of impurities. Chromatographic separation was conducted on an Ultimate XB-C8 column (250 mm  $\times$  4.6 mm  $\times$  5  $\mu\text{m}$ ) under a column oven temperature of 35 °C. The measurement standard was based on European Pharmacopoeia (EP 8.0). Surface morphologies of the PACs were investigated by scanning electron microscopy (SEM, S-4800-I). Energy-dispersive X-ray spectroscopy (EDX) equipped by SEM was used to analyze the content of elements on the AC surface.

The measurements of the surface area and pore size were carried out using  $\text{N}_2$  adsorption–desorption isotherms at  $-196$  °C with a surface area analyzer (TriStar II 3020), and the samples were pretreated at 150 °C under  $\text{N}_2$  atmosphere for 4 h. The Brunauer–Emmett–Teller (BET) equation was used to calculate the BET surface area ( $S_{\text{BET}}$ ) with the instrument's software.<sup>52</sup> The instrument's software also provided the total pore volume, micropore volume ( $V_{\text{mic}}$ ), and pore size distribution by the BJH theory.<sup>53</sup> The mesopore volume ( $V_{\text{mes}}$ ) was calculated from the difference between the total pore volume and the micropore volume ( $V_{\text{T}} - V_{\text{mic}}$ ). The average pore diameter ( $d_p$ ) was calculated using the ratio  $4V_{\text{T}}/S_{\text{BET}}$ .

Surface groups of the PACs were investigated by Fourier transform infrared (FTIR) spectroscopy using a Thermo Scientific Nicolet 6700 spectrophotometer. The samples were mixed with KBr powder and processed in pellets. The number of oxygen acid groups on the material surfaces was determined using the Boehm method,<sup>54</sup> and pH was determined following the method previously reported by Chinese Pharmacopoeia.

Other detailed Tables and Figures can be found in the Supporting Information.

## ■ ASSOCIATED CONTENT

### Supporting Information

The Supporting Information is available free of charge at <https://pubs.acs.org/doi/10.1021/acsomega.0c05637>.

The APAP impurities list; the two mechanisms of the formation of polymers Z2 and Z3; FT-IR spectra of M-T-RAC, O-T-RAC, R-T-RAC and T-RAC; SEM images for T-RAC before and after modified by ammonium sulfate; EDX spectra with the insets of elemental analysis of T-RAC before and after modified by ammonium sulfate, sodium borohydride, hydrogen peroxide;  $\text{N}_2$  adsorption–desorption isotherm and BJH pore size distribution of T-RAC, T-RAC, O-T-RAC, R-T-RAC are provided in Supporting Information Part (PDF)

## ■ AUTHOR INFORMATION

### Corresponding Authors

**Xiaomeng Chu** – College of Chemical & Pharmaceutical Engineering, Hebei University of Science & Technology, Shijiazhuang 050018, P. R. China; [orcid.org/0000-0003-3040-1289](https://orcid.org/0000-0003-3040-1289); Email: [chuxiaomeng@hebest.edu.cn](mailto:chuxiaomeng@hebest.edu.cn)

**Shaojie Liu** – College of Chemical & Pharmaceutical Engineering, Hebei University of Science & Technology, Shijiazhuang 050018, P. R. China; Email: [sjliu16@163.com](mailto:sjliu16@163.com)

### Authors

**Hongjie Liu** – College of Chemical & Pharmaceutical Engineering, Hebei University of Science & Technology, Shijiazhuang 050018, P. R. China

**Yunrui Su** – College of Chemical & Pharmaceutical Engineering, Hebei University of Science & Technology, Shijiazhuang 050018, P. R. China

**Cheng Liu** – College of Chemical & Pharmaceutical Engineering, Hebei University of Science & Technology, Shijiazhuang 050018, P. R. China

**Andi Zhou** – College of Chemical & Pharmaceutical Engineering, Hebei University of Science & Technology, Shijiazhuang 050018, P. R. China

**Xuteng Xing** – College of Chemical & Pharmaceutical Engineering, Hebei University of Science & Technology, Shijiazhuang 050018, P. R. China

**Erjun Tang** – College of Chemical & Pharmaceutical Engineering, Hebei University of Science & Technology, Shijiazhuang 050018, P. R. China

Complete contact information is available at: <https://pubs.acs.org/doi/10.1021/acsomega.0c05637>

### Notes

The authors declare no competing financial interest.

## ■ ACKNOWLEDGMENTS

The financial support for this work was provided by the Natural Science Foundation of Hebei Province (CN) (B2020208069 and B2020208032). Thanks to Jiheng Group (Pharmaceutical) Co., Ltd. for providing the experimental sites, instruments, and a large amount of production data and expertise. Special thanks to Dr. Shangjin Yang for his kind supervision and help in this project.

## REFERENCES

- (1) de Luna, M. D. G.; Briones, R. M.; Su, C. C.; Lu, M. C. Kinetics of acetaminophen degradation by fenton oxidation in a fluidized-bed reactor. *Chemosphere* **2013**, *90*, 1444–1448.
- (2) Li, Y.; Jin, H.; Liu, W.; Su, H.; Lu, Y.; Li, J. Study on regeneration of waste powder activated carbon through pyrolysis and its adsorption capacity of phosphorus. *Sci. Rep.* **2018**, *8*, No. 778.
- (3) Li, Q.; Qi, Y.; Gao, C. Chemical regeneration of spent powdered activated carbon used in decolorization of sodium salicylate for the pharmaceutical industry. *J. Cleaner Prod.* **2015**, *86*, 424–431.
- (4) Zhou, E.; He, Y.; Ma, X.; Liu, G.; Huang, Y.; Chen, C.; Wang, W. Study of the combination of sulfuric acid treatment and thermal regeneration of spent powdered activated carbons from decolourization process in glucosamine production. *Chem. Eng. Process.: Process Intensification* **2017**, *121*, 224–231.
- (5) Ledesma, B.; Román, S.; Álvarez-Murillo, A.; Sabio, E.; González, J. F. Cyclic adsorption/thermal regeneration of activated carbons. *J. Anal. Appl. Pyrol.* **2014**, *106*, 112–117.
- (6) Han, X.; Lin, H.; Zheng, Y. Regeneration methods to restore carbon adsorptive capacity of dibenzothiophene and neutral nitrogen heteroaromatic compounds. *Chem. Eng. J.* **2014**, *243*, 315–325.
- (7) Lu, P. J.; Lin, H. C.; Yu, W. T.; Chern, J. M. Chemical regeneration of activated carbon used for dye adsorption. *J. Taiwan Inst. Chem. Eng.* **2011**, *42*, 305–311.
- (8) Guo, D.; Shi, Q.; He, B.; Yuan, X. Different solvents for the regeneration of the exhausted activated carbon used in the treatment of coking wastewater. *J. Hazard. Mater.* **2011**, *186*, 1788–1793.
- (9) Scamehorn, J. F. Removal of vinyl chloride from gaseous streams by adsorption on activated carbon. *Ind. Eng. Chem. Process Des. Dev.* **1979**, *18*, 210–217.
- (10) Urano, K.; Yamamoto, E.; Takeda, H. Regeneration rates of granular activated carbons containing adsorbed organic matter. *Ind. Eng. Chem. Process Des. Dev.* **1982**, *21*, 180–185.
- (11) Foo, K. Y.; Hameed, B. H. A rapid regeneration of methylene blue dye-loaded activated carbons with microwave heating. *J. Anal. Appl. Pyrol.* **2012**, *98*, 123–128.
- (12) Cherbański, R. Regeneration of granular activated carbon loaded with toluene-Comparison of microwave and conductive heating at the same active powers. *Chem. Eng. Process.: Process Intensification* **2018**, *123*, 148–157.
- (13) El Gamal, M.; Mousa, H. A.; El-Naas, M. H.; Zacharia, R.; Judd, S. Bio-regeneration of activated carbon: a comprehensive review. *Sep. Purif. Technol.* **2018**, *197*, 345–359.
- (14) Yap, P. S.; Lim, T. T. Solar regeneration of powdered activated carbon impregnated with visible-light responsive photocatalyst: Factors affecting performances and predictive model. *Water Res.* **2012**, *46*, 3054–3064.
- (15) Chu, L.; Wang, J. Regeneration of sulfamethoxazole-saturated activated carbon using gamma irradiation. *Radiat. Phys. Chem.* **2017**, *130*, 391–396.
- (16) Sun, Y.; Zhang, B.; Zheng, T.; Wang, P. Regeneration of activated carbon saturated with chloramphenicol by microwave and ultraviolet irradiation. *Chem. Eng. J.* **2017**, *320*, 264–270.
- (17) Tanthapanichakoon, W.; Ariyadejwanich, P.; Japthong, P.; Nakagawa, K.; Mukai, S. R.; Tamon, H. Adsorption-desorption characteristics of phenol and reactive dyes from aqueous solution on mesoporous activated carbon prepared from waste tires. *Water Res.* **2005**, *39*, 1347–1353.
- (18) Zhang, H. Regeneration of exhausted activated carbon by electrochemical method. *Chem. Eng. J.* **2002**, *85*, 81–85.
- (19) Salvador, F.; Martinsanchez, N.; Sanchezhernandez, R.; Sanchezmontero, M. J.; Izquierdo, C. Regeneration of carbonaceous adsorbents. Part II: Chemical, Microbiological and Vacuum Regeneration. *Micropor. Mesopor. Mat.* **2015**, *202*, 277–296.
- (20) Mcquillan, R. V.; Stevens, G. W.; Mumford, K. A. The electrochemical regeneration of granular activated carbons: A review. *J. Hazard. Mater.* **2018**, *355*, 34–49.
- (21) Grant, T. M.; King, C. J. Mechanism of irreversible adsorption of phenolic compounds by activated carbon. *Ind. Eng. Chem. Res.* **1990**, *29*, 264–271.
- (22) Lu, Q.; Sorial, G. A. Adsorption of phenolics on activated carbon-impact of pore size and molecular oxygen. *Chemosphere* **2004**, *55*, 671–679.
- (23) Vidic, R. D.; Tessmer, C. H.; Uranowski, L. J. Impact of surface properties of activated carbons on oxidative coupling of phenolic compounds. *Carbon* **1997**, *35*, 1349–1359.
- (24) Tessmer, C. H.; Vidic, R. D.; Uranowski, L. J. Impact of oxygen-containing surface functional groups on activated carbon adsorption of phenols. *Environ. Sci. Technol.* **1997**, *31*, 1872–1878.
- (25) Terzyk, A. P. Further insights into the role of carbon surface functionalities in the mechanism of phenol adsorption. *J. Colloid Interface Sci.* **2003**, *268*, 301–329.
- (26) Lawal, I. A.; Chetty, D.; Akpotu, S. O.; Moodley, B. Sorption of Congo red and reactive blue on biomass and activated carbon derived from biomass modified by ionic liquid. *Environ. Nanotechnol. Monit. Manag.* **2017**, *8*, 83–91.
- (27) Fang, R.; Huang, H.; Huang, W.; Ji, J.; Feng, Q.; Shu, Y.; Xie, R.; et al. Influence of peracetic acid modification on the physicochemical properties of activated carbon and its performance in the ozone-catalytic oxidation of gaseous benzene. *Appl. Surf. Sci.* **2017**, *420*, 905–910.
- (28) Cheng, S.; Zhang, L.; Ma, A.; Xia, H.; Peng, J.; Li, C.; Shu, J. Comparison of activated carbon and iron/cerium modified activated carbon to remove methylene blue from wastewater. *J. Environ. Sci.* **2018**, *65*, 92–102.
- (29) Yao, X.; Liu, J.; Gong, G.; Jiang, Y.; Xie, Q. Preparation and modification of activated carbon for benzene adsorption by steam activation in the presence of KOH. *Int. J. Mining Sci. Technol.* **2013**, *23*, 395–401.
- (30) Que, W.; Jiang, L.; Wang, C.; Liu, Y.; Zeng, Z.; Wang, X.; Liu, S.; et al. Influence of sodium dodecyl sulfate coating on adsorption of methylene blue by biochar from aqueous solution. *J. Environ. Sci.* **2018**, *70*, 166–174.
- (31) Gokce, Y.; Aktas, Z. Nitric acid modification of activated carbon produced from waste tea and adsorption of methylene blue and phenol. *Appl. Surf. Sci.* **2014**, *313*, 352–359.
- (32) Fang, R.; Huang, H.; Huang, W.; Ji, J.; Feng, Q.; Shu, Y.; Xie, R.; et al. Influence of peracetic acid modification on the physicochemical properties of activated carbon and its performance in the ozone-catalytic oxidation of gaseous benzene. *Appl. Surf. Sci.* **2017**, *420*, 905–910.
- (33) Pereira, M. F. R.; Soares, S. F.; Órfão, J. J.; Figueiredo, J. L. Adsorption of dyes on activated carbons: influence of surface chemical groups. *Carbon* **2003**, *41*, 811–821.
- (34) Radhika, R.; Jayalatha, T.; Jacob, S.; Rajeev, R.; George, B. K.; Anjali, B. R. Removal of perchlorate from drinking water using granular activated carbon modified by acidic functional group: adsorption kinetics and equilibrium studies. *Process Saf. Environ.* **2017**, *109*, 158–171.
- (35) Dąbrowski, A.; Podkościelny, P.; Hubicki, Z.; Barczak, M. Adsorption of phenolic compounds by activated carbon—a critical review. *Chemosphere* **2005**, *58*, 1049–1070.
- (36) Sobiesiak, M. Chemical Structure of Phenols and its Consequence for Sorption Processes. In *Phenolic Compounds-Natural Sources, Importance and Applications*; 2017.
- (37) Moreno-Castilla, C.; Ferro-García, M. A.; Joly, J. P.; Bautista-Toledo, I.; Carrasco-Marin, F.; Rivera-Utrilla, J. Activated carbon surface modifications by nitric acid, hydrogen peroxide, and ammonium peroxydisulfate treatments. *Langmuir* **1995**, *11*, 4386–4392.
- (38) Xue, Y.; Gao, B.; Yao, Y.; Inyang, M.; Zhang, M.; Zimmerman, A. R.; et al. Hydrogen peroxide modification enhances the ability of biochar (hydrochar) produced from hydrothermal carbonization of peanut hull to remove aqueous heavy metals: batch and column tests. *Chem. Eng. J.* **2012**, *200*–202, 673–680.

(39) Budarin, V. L.; Clark, J. H.; Mikhalovsky, S. V.; Gorlova, A. A.; Boldyreva, N. A.; Yatsimirsky, V. K. The hydrophobisation of activated carbon surfaces by organic functional groups. *Adsorpt. Sci. Technol.* **2000**, *18*, 55–64.

(40) Nematollahi, D.; Shayani-Jam, H.; Alimoradi, M.; Niroomand, S. Electrochemical oxidation of acetaminophen in aqueous solutions: Kinetic evaluation of hydrolysis, hydroxylation and dimerization processes. *Electrochim. Acta* **2009**, *54*, 7407–7415.

(41) Potter, D. W.; Miller, D. W.; Hinson, J. A. Identification of acetaminophen polymerization products catalyzed by horseradish peroxidase. *J. Biol. Chem.* **1985**, *260*, 12174–12180.

(42) Rao, B. V. S. K.; Mouli, K. C.; Rambabu, N.; et al. Carbon-based solid acid catalyst from de-oiled canola meal for biodiesel production. *Catal. Commun.* **2011**, *14*, 20–26.

(43) Mukherjee, A.; Zimmerman, A. R.; Harris, W. Surface chemistry variations among a series of laboratory-produced biochars. *Geoderma* **2011**, *163*, 247–255.

(44) Lu, J.; Huang, Q.; Mao, L. Removal of acetaminophen using enzyme-mediated oxidative coupling processes: I. Reaction rates and pathways. *Environ. Sci. Technol.* **2009**, *43*, 7062–7067.

(45) Peng, A.; Huang, M.; Chen, Z.; Gu, C. Oxidative coupling of acetaminophen mediated by Fe<sup>3+</sup>-saturated montmorillonite. *Sci. Total Environ.* **2017**, *595*, 673–680.

(46) Vega, E.; Valdés, H. New evidence of the effect of the chemical structure of activated carbon on the activity to promote radical generation in an advanced oxidation process using hydrogen peroxide. *Microporous Mesoporous Mater.* **2018**, *259*, 1–8.

(47) Doucet, F. J.; Mohamed, S.; Neyt, N.; Castleman, B. A.; et al. Thermochemical processing of a South African ultrafine coal fly ash using ammonium sulphate as extracting agent for aluminium extraction. *Hydrometallurgy* **2016**, *166*, 174–184.

(48) Hameed, B. H.; Tan, I. A. W.; Ahmad, A. L. Optimization of basic dye removal by oil palm fibre-based activated carbon using response surface methodology. *J. Hazard. Mater.* **2008**, *158*, 324–332.

(49) Deng, H.; Yang, L.; Tao, G. H.; Dai, J. L. Preparation and characterization of activated carbon from cotton stalk by microwave assisted chemical activation - application in methylene blue adsorption from aqueous solution. *J. Hazard. Mater.* **2009**, *166*, 1514.

(50) Galhetas, M.; Mestre, A. S.; Pinto, M. L.; Gulyurtlu, I.; Lopes, H.; Carvalho, A. P. Carbon-based materials prepared from pine gasification residues for acetaminophen adsorption. *Chem. Eng. J.* **2014**, *240*, 344–351.

(51) Zhan, J.; Wang, Y.; Wang, H.; Shen, W.; Pan, X.; Wang, J.; et al. Electro-peroxone regeneration of phenol-saturated activated carbon fiber: the effects of irreversible adsorption and operational parameters. *Carbon* **2016**, *109*, 321–330.

(52) Steele William, A. *Adsorption Surface Area and Porosity*, 2nd ed.; Gregg, S. J.; Sing, K. S. W., Eds.; Academic Press, 1982; p 312.

(53) Liu, C.; Sun, Y.; Wang, D.; Sun, Z.; Chen, M.; Zhou, Z.; Chen, W. Performance and mechanism of low-frequency ultrasound to regenerate the biological activated carbon. *Ultrason. Sonochem.* **2017**, *34*, 142–153.

(54) Boehm, H. P. Surface oxides on carbon and their analysis: a critical assessment. *Carbon* **2002**, *40*, 145–149.